

A population-based incremental learning algorithm to identify optimal location of left-turn restrictions in urban grid networks

Murat Bayrak^a, Zhengyao Yu^b, and Vikash V. Gayah^b

^aAalto University, 341b Otakaari 4, Espoo, Finland

^bThe Pennsylvania State University, 201 Transportation Research Building, State College, PA, USA

ARTICLE HISTORY

Compiled August 9, 2021

ABSTRACT

The treatment of left turns at signalized intersections drives the development of signal phasing and timing plans and also plays an important role in overall traffic network operations. Accommodating left turns allows for the most direct routing but reduces intersection capacity, whereas restricting left turns improves capacity but requires some vehicles to travel longer distances. This paper proposes a population-based incremental learning (PBIL) algorithm to determine at which intersections left-turn restrictions should be enacted to maximize a network's operational performance. The performance of each configuration is tested in a micro-simulation environment on both perfect and imperfect square grid networks. Comparison with a partial enumeration of feasible options reveals that the PBIL algorithm is effective at identifying a near-optimal configuration of left-turn restrictions. The resulting configurations suggest that left turns should be generally restricted at intersections that carry the most flow. These intersections typically occur in the central portion of the network when demands are relatively uniform. Doing so helps to provide additional intersection capacity at the locations where it is most necessary, while minimizing the additional travel distance that is incurred due to detours caused by the left-turn restrictions. These provide insight as to how urban traffic networks might be managed to improve network efficiency by only enacting left-turn restrictions at a subset of locations.

KEYWORDS

conflicting left-turns; urban network design; left-turn restrictions; optimal spatial configuration; population-based incremental learning

1. Introduction

The treatment of conflicting left-turns at signalized intersections is one of the driving factors in the development of Signal Phasing and Timing (SPaT) plans (Roess, Prassas, and McShane 2010; Cottrell 1985). These left turns present significant safety issues as turning vehicles must cross the path of opposing through vehicles to traverse the intersection. Serving left turns in a permitted fashion is risky as drivers need to identify appropriate gaps in the opposing traffic in which to move. If sufficient gaps do not exist, the left-turning vehicles may block other vehicles on the same approach from discharging (Fambro, Messer, and Andersen 1977). Even if dedicated left-turn pock-

ets are installed to separate turning vehicles, queued left-turn vehicles can spillover and reduce the rate at which other vehicles can discharge (Haddad and Geroliminis 2013). Providing protected left-turn phases can completely eliminate conflicts between turning and through vehicles. However, doing so reduces total intersection capacity by taking time away from through movements and introducing additional lost times during which the intersection is not serving any vehicles (Messer and Fambro 1977; Newell 1959). Both treatments can be provided in consecutive phases in a protected-permitted fashion, but doing so still may reduce intersection capacity due to left-turn queues and additional lost times incurred.

Alternative intersection designs have been proposed to facilitate conflicting left turns at signalized intersections in non-traditional ways. These rely on changing the geometry of the intersection or additional infrastructure elements (e.g., more lanes, quadrant roadways or installation of midblock signals) to reorganize conflicts between vehicles and increase intersection efficiency (Chowdhury 2011; Hummer 1998; Hughes et al. 2010; Berkowitz, Bragdon, and Mier 1996; Reid and Hummer 2001; Xuan et al. 2012; Xuan, Daganzo, and Cassidy 2011; Zhao et al. 2013; Zhao, Liu, and Wang 2016). However, these designs often require large spatial footprints or additional infrastructure elements. Thus, implementation of these designs can be costly or may not be suitable for dense urban environments. For example, tandem intersections and exit-lanes require pre-signals that can only be implemented on longer blocks, while special width approach lanes require wider footprints that might not be available in urban areas. Some of these designs do not completely eliminate left turning conflicts, while others—like the median U-turns—move conflicts to midblock locations.

Another approach is to eliminate the conflicts altogether by restricting all left-turning movements at an intersection. Doing so allows for simpler signal phasing and allows the intersection to operate more efficiently. However, this comes with the cost of added travel distance for vehicles that would otherwise make a left turn. Recent analytical and simulation studies have examined the network-wide impacts of eliminating left-turns at intersections (Gayah and Daganzo 2012; Ortigosa, Menendez, and Gayah 2015; Ortigosa, Gayah, and Menendez 2019; DePrator, Hitchcock, and Gayah 2017; Ortigosa and Menendez 2014) using developed network-wide measures of performance (Daganzo 2007). These studies show that eliminating left-turns from all intersections in a network can improve the maximum rate that trips are served by up to 33% compared with networks that allow left turns and that left turns restrictions could be lifted in light traffic conditions when the additional capacity is not needed. However, these studies only focus on eliminating left turns network-wide and do not consider how to apply this treatment at individual intersections.

Very few studies have examined the application of left turn restrictions or alternative left-turn treatments at individual intersections on a network, perhaps due to the complexity of the problem. For one, the solution space is incredibly large. A network with N intersections and D decisions per intersection would have D^N potential configurations that would need to be assessed. Additionally, the solutions have interdependencies that need to be addressed. Changes in left-turn treatments at one intersection directly influence operations at neighbouring intersections. Additionally, the treatments will influence how vehicles route themselves in the network. For these reasons, the problem typically cannot be expressed as a traditional mathematical program. Several recent studies proposed generic methodologies to identify intersections that should restrict left turns, but relied on very simplistic traffic models that do not accurately account for vital traffic dynamics such as queue spillbacks at neighbouring intersections and vehicle routing in response to the changes (Tang and Friedrich

2016). Other studies adopted a bi-level optimization approach to capture the changes in the route selection behavior of the drivers (Long, Szeto, and Huang 2014; Liu and Luo 2012; Tang and Friedrich 2018; Tang 2019; Tang, Liu, and Friedrich 2019). However, these studies also used a simple traffic model that cannot account the effects of queue spillbacks. This accuracy problem of the exiting bi-level methodologies can be solved by using simulation. Two studies used simulation to examine the effectiveness of pre-specified left-turn treatments spatially within a network (Hajbabaie, Medina, and Benekohal 2010; Chowdhury et al. 2005). However, these studies did not optimize where the left-turn treatment should be enacted.

In light of this, the purpose of this paper is to propose a method to more generally identify intersection locations (if any) at which left turns should be restricted in dense, grid-like urban networks. A microscopic simulation platform was used to simulate the behaviour of vehicles on these networks to account for traffic dynamics and queue spillbacks that might influence intersection operations, along with dynamic vehicle routing in response to the left-turn treatments. A population-based incremental learning (PBIL) algorithm (Baluja 1994) is proposed to determine the optimal location to implement left-turn restrictions within a network. The results of the PBIL algorithm was compared to a partial enumeration of all options to verify that the PBIL was able to obtain a reasonable solution that accurately captured the spatial traffic dynamics associated with the problem. Examination of the configurations identified by the PBIL method suggests that there exists a general reproducible spatial pattern of left-turn restrictions that minimizes travel times and maximizes network efficiency, and that left-turn restrictions should generally be enacted at intersections that carry the largest total flows and have lower ratios of left-turning vehicles.

The remainder of this paper is organized as follows. First, the network set-up and optimization methodologies used are introduced. Then, the optimization results to obtain the spatial configuration of left-turn restrictions are discussed when the enumeration and PBIL approaches are applied to a perfect grid network. This includes the best-performing configurations for a single simulation instance, as well as the best-performing configuration across multiple simulation instances. Next, the optimization results are extended to imperfect grid networks that are more readily observed in practice. Finally, concluding remarks are provided.

2. Methodology

This section describes the methods that were used in this paper to determine where left-turns should be restricted spatially across an urban network. We first introduce the network settings used in this work, and then discuss the two optimization approaches applied. The first is population-based incremental learning (PBIL), which is a general genetic optimization method that can be applied network optimization problems like this one. The second is a brute-force enumeration, which is used to assess the effectiveness of PBIL at solving this problem.

2.1. *Network set-up*

Traffic network performance under various left-turn restriction configurations was tested using the Aimsun micro-simulation platform. The micro-simulation was used since it simulates the behaviour of all individual network elements (e.g., vehicles and traffic signals) and can accurately capture relevant urban traffic phenomena such as

congestion propagation/queue spillbacks, vehicle routing, and heterogeneous driver behaviour. As will be described later in this section, the simulation must be run many times under various settings to determine the optimal left-turn restriction configuration. To facilitate this, Python scripts were created to generate the various network configurations automatically and the simulations were run using Aimsun's console mode, which significantly reduces runtime. In this way, a specific solution could be tested for a single simulation instance in the order of seconds.

In this paper, we simulate square grid networks due to its simplicity and generality. While real urban street networks are rarely perfect square grids, many street networks have a grid-like structure and thus studying this network structure can provide insights that are more generalizable to other networks compared to other network structures; see e.g., (Ortigosa, Gayah, and Menendez 2019; Ortigosa and Menendez 2014; Knoop, Hoogendoorn, and Van Lint 2012; Mazloumian, Geroliminis, and Helbing 2010). Both perfect and imperfect grid structures will be considered in this work. We specifically focus on 8x8 grid network in which vehicles are allowed to enter/exit the network at both internal and periphery locations. All streets in the network were assumed to have two-way operation and were comprised of two travel lanes in each direction. Each street was coded as an arterial, with a capacity of 1600 veh/hr and a speed limit of 48 km/hr (30 mi/hr). Block lengths were set to 250 m (820 ft).

All 64 intersections in the network were signalized and shared a common cycle length of 90 seconds¹. At each intersection, two left-turn treatment options were considered: accommodating left-turns using permitted phasing or completely restricting left-turns at all approaches. Permitted phasing was chosen since it is commonly applied in urban environments and does not require a dedicated left-turn lane or left-turn pocket. In this way, restricting left turns does not require that some lanes/infrastructure goes unused. However, simulation tests reveal that the proposed methods can be applied to situations in which protected left-turn phasing is used instead. In both cases, a two-phase scheme was applied in which each direction received 42 seconds of green and a 3-second clearance and change interval was applied between consecutive phases. Offsets between adjacent signals were set to zero as a recent study found that offsets had minimal advantages to overall network-wide operations in two-dimensional grid networks (Girault et al. 2016). Left-turning vehicles were assumed to share the left lane with through vehicles at intersections at which left turns were permitted. It is also assumed that left-turn restrictions are never applied at the intersections in the corner of the network. This helps to ensure that a feasible path is available between all OD pairs in the simulation. In practice, this latter assumption may not be necessary since other routes outside of the simulated network may be available to serve these OD pairs; however, these alternatives would likely increase travel distance and thus may not be used.

Origins and destinations were placed at all 32 entry/exit points on the periphery of the network (8 on each side), as well as at the mid-block points of all internal links. A uniform demand pattern was considered in which each origin-destination pair was expected to exchange the same number of trips on average. However, the actual number of trips exchanged during any specific simulation instance was subject to randomness in the Aimsun simulation environment, so the realized demand pattern was never exactly uniform during any one simulation instance. This randomness was also leveraged to examine the robustness of the optimal left-turn configuration across

¹Note that the selection of this cycle length do not change the overall trends and patterns. The optimization process was repeated for different cycle lengths and the same general patterns were obtained.

all intersections.

Vehicles were routed using the stochastic c-logit route choice model native to the Aimsun micro-simulation software. This routing pattern aims to mimic a stochastic user-equilibrium routing solution in which vehicles make routing decisions to minimize their own personal travel costs, which is assumed to be made up of prevailing travel times and unobserved error terms that reflect user preferences. The routing decisions are made at the time a trip is created and vehicles select their routing based on the average travel time on links over the past 3 minutes. However, a subset (50%) of vehicles was assumed to be able to change their routes mid-trip based on prevailing traffic patterns. This re-routing occurred at regular intervals of 3 minutes. This “adaptive” routing was considered as previous research showed that intelligent re-routing was able to provide better network-wide operational performance (Gayah and Daganzo 2011; Daganzo, Gayah, and Gonzales 2011; Gayah, Gao, and Nagle 2014; Saberi, Mahmassani, and Zockaei 2014).

A constant demand pattern was considered in which an average of 367 total trips per minute was simulated for 45 minutes, followed by a recovery period of 15 minutes to ensure that all vehicles were able to exit the network by the end of the simulation. Under this demand, the network became slightly congested when left turns were accommodated at all intersections. Cumulative count curves of vehicle entries and exits (i.e., arrivals to their destination) were used to determine the total travel time associated with each spatial configuration of left-turn restrictions. The total travel time was used as the primary metric to rank configurations and identify the optimal solution. Note that this total travel time metric also included additional travel time due to vehicles having to travel longer distances imparted due to left turn restrictions.

2.2. *Optimization of left-turn restriction configurations*

Two methods were used to identify the optimal spatial configuration of left-turn restrictions. The first was a brute-force enumeration approach, which was used to identify the best configuration in a subset of all possible symmetrical spatial configurations. The second was a heuristic optimization algorithm known as population-based incremental learning (PBIL). The remainder of this section outlines these two approaches.

2.2.1. *Method 1: Population-based incremental learning (PBIL)*

In this paper, a heuristic method—population-based incremental learning (PBIL)—is proposed to determine the optimal left-turn restriction configuration. PBIL combines the mechanisms of both genetic algorithms with competitive learning (Baluja 1994) and has been shown to outperform traditional genetic algorithms in both speed and solution accuracy. Furthermore, PBIL also better addresses situations in which epistasis exists, which means that there are meaningful interactions between individual elements in a solution (Reeves and Wright 1995). For example, in the left-turn restriction problem considered here, the existence of a left-turn restriction at any one intersection will impact vehicle arrivals to and, thus, the performance of, neighbouring intersections. Therefore, the method has the potential to solve a wide range of traffic network optimization problems.

In this particular problem where the solution is a set of binary decision variables (representing whether or not to restrict left-turns at each intersection), the PBIL algorithm works as follows:

Step 0. A vector, P^1 , is defined with a number of elements equal to the number of binary components in the solution. In our problem, this is the number of signalized intersections for which left-turn restrictions will be considered. As explained in the network setup section, all intersections except the intersections at the corners of the network are considered for left-turn restrictions. Each element $P_i^1 \in P$ represents the probability that a given intersection i will have left-turns restricted. This probability vector is initialized such that each element is equal to 0.5. Set $t = 1$ where t is an index for the current generation in the optimization algorithm.

Step 1. A population of N candidate solutions is generated using the probability vector P^t to assign binary decisions to each of the solution components. In our problem, this means left-turn restrictions are randomly determined at each intersection using the probabilities in P^t .

Step 2. The fitness of each solution is determined. In this problem, the total travel time is the measurement used to assign this fitness. The best (b^t) and worst (w^t) solutions are identified based on this fitness score.

Step 3. A new probability vector is determined (P^{t+1}) using the current probability vector and applying positive learning, negative learning, and mutation.

- Positive learning: Equation 1 updates the solution by learning from and adapting features of the best-performing solution.

$$P_i^{t+1} = P_i^t \times (1 - LR^+) + b_i^t \times LR^+ \quad (1)$$

where LR^+ is a number between 0 and 1 and represents the amount that is learned from the best solution.

- Negative learning: if the best and worst solutions are not equal ($b^t \neq w^t$), Equation 2 updates the solution by learning from and avoiding features of the worst-performing solution.

$$P_i^{t+1} = P_i^t \times (1 - LR^-) + w_i^t \times LR^- \quad (2)$$

where LR^- is a number between 0 and 1 and represents the amount that is learned from the worst solution.

- Mutation: random changes are made within the solution to help avoid the algorithm getting stuck within a locally optimal solution. With random probability m , known as the mutation rate, Equation 3 shifts the individual probabilities in the probability vector.

$$P_i^{t+1} = P_i^t \times (1 - \Delta m) + rand(0, 1) \times \Delta m \quad (3)$$

where Δm is the magnitude of the random mutation (mutation shift) and $rand(0, 1)$ is a random binary number.

Step 4. Check for convergence.

- If $P_i^t = P_i^{t+1}$ for over 90% of elements in P , end algorithm.
- Otherwise, increment t and go back to Step 1.

In this paper, the PBIL algorithm was implemented using the following parameters:

- $N = 50$
- $LR^+ = 0.1$
- $LR^- = 0.075$

- $P_m = 0.02$
- $\Delta m = 0.05$

2.2.2. Method 2: Brute-force enumeration

To verify the solutions obtained from the PBIL method, a brute-force enumeration of a subset of the feasible set of options is also performed. Since there are 64 intersections in the 8×8 grid network considered, there are $2^{64} \approx 1.8 \times 10^{19}$ unique cases that must be considered, which is not tractable. To make the problem computationally possible, we make some simplifying assumptions in the perfect grid network case to reduce the number of potential solutions that must be considered when applying brute-force enumeration.² First, we assume that solutions must be rotationally symmetric around the center of the network. The assumption of a symmetric solution is reasonable since we consider here a perfect grid network structure with a uniform average demand pattern. And, the solution is likely to be rotationally symmetric due to the way in which left-turn restrictions would change how vehicles are routed in the network. Therefore, we only focus on spatial left-turn restriction configurations within a 4×4 quadrant of the 8×8 network and apply this configuration rotationally to the other quadrants. This reduces the number of potential configurations that must be tested to $2^{16} = 65,536$, which is a much more manageable number. The assumption of always allowing left-turns at the corners of the network further reduces the total number of configurations to $2^{15} = 32,768$.

3. Optimal spatial configuration for perfect grid network

In this section, the methods previously described are applied to determine the optimal spatial configuration for left-turn restrictions on a perfect square grid network. First, we focus on the optimal configuration for a single simulation instance. This is a specific realization of the average demands that were used and could represent the demands experienced on one specific day during a set of typical days. Then, we focus on the best-performing configuration across multiple simulation instances individually (i.e., configuration that works best on each individual day) and collectively (configuration that works best across all days combined). The latter is important to identify the configuration that is most robust to fluctuations in travel patterns that might occur on a day-to-day basis, even when travel demands are generally the same.

3.1. Enumeration configuration

First, the entire set of 32,768 candidate configurations were simulated for a single simulation instance to identify the best-performing network configuration. Figure 1 provides a graphical depiction of the total travel times obtained from the configurations ranked from best (left-most side) to worst (right-most side). As shown, the travel times range from a worst of about 5.25×10^6 total vehicle-sec to a best of about 3.72×10^6 total vehicle-sec. The slope of this plot represents the amount of travel time added by going from a specific configuration to the next-worst configuration.

²Note that these assumptions can be readily relaxed when applying the PBIL algorithm and are only made to directly compare the results obtained with the PBIL algorithm with the brute-force enumeration. The adoption of this assumption does not imply that the authors believe this assumption should be made for real world scenarios.

Note that the plot is relatively flat in the middle portion of the figure, which covers about 75 percent of the configurations. This suggests that most configurations have similar total travel time in this range. The curve is much steeper at the left- and right-hand sides. This suggests that at the best- and the worst-performing configurations, the change in travel time can be significant when moving between similarly-ranked options. The inset of Figure 1 magnifies this curve for the 1000 best-performing configurations. It suggests that the top-performing 50 configurations (indicated by the red line) greatly outperform the others. The cases where left-turns are permitted at all intersections (PLT) and are restricted at all intersections (RLT) are also indicated in the figure. These cases perform 5.6% and 15.6% worse than the best-performing left-turn restriction configuration. Note that accommodating left turns at all intersections outperforms restricting left turns at all intersections due to moderate traffic demand in the network; under these conditions, it is not necessary to prohibit left turns everywhere since some intersections are undersaturated.

[FIGURE 1 HERE]

[FIGURE 2 HERE]

Figure 2 illustrates the commonalities between the top-performing 50, 100 and 1000 configurations based on this enumeration approach using heat-maps that show the frequency of left-turn restrictions being applied at each intersection in each subset of solutions. Larger and more yellow dots indicate a higher frequency of left-turn restrictions being applied, while smaller and more blue dots indicate a lower frequency. Note that the heat-maps are rotationally symmetric due to the assumption made to make the brute-force enumeration feasible. A review of these heat-maps reveals that the likelihood that a left-turn restriction is implemented at any intersection in the top-performing configurations generally decreases with the distance between that intersection and the center of the network. A majority (over 85%) of the top configurations across each of the subset of best 50, 100 or 1000 configurations implement left-turn restrictions in the central portions of the network, and only about 10% of these configurations implement left-turn restrictions at intersections on the periphery.

One reason for this is that intersections in the central portion of the network generally carry higher flows than those in the periphery and also have a lower fraction of vehicles wishing to make a left turn; see the left-hand side of Figure 3 which provides an illustration of total traffic volumes and left-turn ratio for the case when left turns are accommodated at all intersections. Restricting left turns at these central intersections increases the capacity for vehicle throughput by removing the presence of queued left-turning vehicles waiting for a gap in opposing traffic. While restricting left turns causes vehicles to travel longer distances, only a small proportion of the vehicles using these intersections should be impacted since the ratio of left-turning vehicles at these intersections is relatively small. Furthermore, previous work has shown that vehicles are often able to re-route without any additional travel distance if left-turns are accommodated at other intersections in the network (Yu and Gayah 2018, 2019). To this end, the average total distance travelled is approximately the same across the set of top-performing 50, 100 and 1000 configurations (approximately $2.67 \times 10^7 m$) and this represents only a modest increase of 2.8% over the configuration with the smallest total travel distance. Left-turn restrictions are less likely at intersections on the periphery since these generally carry much lower flows. The additional capacity that can be provided at these locations by enacting left turn restrictions is not needed or used. At these locations, the turning ratios are higher and any additional travel

distance quickly offsets the capacity gain since the latter is generally unused. Thus, the best-performing configurations tend to provide the highest capacity at the intersections that serve the highest flows and accommodates left turns at intersections with fairly high left-turning ratios; see the right-hand side of Figure 3 which provides an illustration of total traffic volumes and left-turn ratio for the best-performing left-turn restriction configuration case.

[FIGURE 3 HERE]

Notice also that a small portion of the top-performing configurations (approximately 15%) do not implement left-turn restrictions at the central intersections. A quick review of these configurations suggests that these generally have left-turn restrictions at intersections in the immediately adjacent intersections (i.e., along the periphery of the central 4×4 section of the network). Thus, there is still an overall trend of left-turn restrictions in the central portion of the network.

3.2. *PBIL configuration*

With all the candidate network configurations simulated already in the previous subsection, we now apply the PBIL optimization algorithm to assess how well it can identify the best-performing left-turn restriction configuration. For a fair comparison with the enumerated results, the same random seed is used in the PBIL and only rotationally symmetric configurations are considered in the PBIL. Since the PBIL is a heuristic method and the final solution is subject to the inherent randomness of the process, the algorithm was run twice to provide a fairer comparison. The top of Figure 4 3 provides a plot of the minimum and maximum total travel time obtained from the best and worst configurations for each generation. As shown, these values start out with a very wide difference of about 1×10^6 sec in the first generation since all configurations tested are randomly generated in the beginning. However, through a combination of positive/negative learning and random mutation, the best- and worst-performing solutions start to converge and continue to do so until generation 18 (first instance) and generation 17 (second instance) when the difference is only about 1×10^5 sec and the algorithm eventually converges. The bottom of Figure 4 provides the best-performing configurations of left-turn restrictions obtained from the two PBIL instances. Examining the configurations in detail, we see that both identified solutions have left-turn restrictions in the central portion of the network and very few left-turn restrictions on the periphery. This is consistent with the enumeration results.

When compared to the list of enumeration results, the two configurations identified by the PBIL algorithm represent the 10th- and 17th-best configurations out of 32,768 possible options. The performance gap between these two identified solutions and the best solution obtained through enumeration is 1.7% and 1.9%, respectively. This suggests that the PBIL algorithm is capable of accurately obtaining a reasonably good configuration for left-turn restrictions in a grid network, even with the interdependencies between the decisions at each intersection. Furthermore, the PBIL requires many fewer simulation tests than the brute-force enumeration. When the best-performing solution is obtained within 22 generations, only 1,110 simulation runs are needed to be performed with a population size of 50, compared with the 32,768 simulation runs required for the partial enumeration.

Note that these results assume that configurations are rotation symmetric. This was only assumed to compare the results with the brute-force enumeration, which is infea-

sible to apply for asymmetric cases. Simulation runs were also performed to examine how much more travel time could be improved by relaxing the symmetry constraint in the PBIL algorithm. The results revealed that travel time could be further improved by up to 0.94% (to a total travel time of 3.68×10^6 sec) when this constraint was relaxed. Note that the improvement is rather modest and is likely due to asymmetries in the realized demand pattern for the given simulation random seed since the network structure and overall demand pattern is symmetric. Thus, this symmetry assumption will be maintained for the analysis of a perfect grid in the remainder of this section. However, Section 4 will relax this assumption when imperfect grids are considered.

[FIGURE 4 HERE]

3.3. *Performance of individual random seeds*

The previous results considered the optimal left-turn restriction configuration for just a single simulation instance that had a specific trip generation sequence and OD pattern. The PBIL algorithm was found capable of identifying the best-performing network configurations. However, results from a single instance is insufficient as traffic patterns change constantly. We now consider the optimal configuration for multiple simulation instances (e.g., multiple individual days) individually to examine consistency in the spatial configuration of left-turn restrictions under stochastic demands.

Both the brute-force enumeration and PBIL approaches were repeated for nine unique simulation instances. To reduce the computational complexity in the enumeration approach, only the top-performing 2,000 solutions from the first instance were tested for the remaining instances. Random checks of the remaining configurations indicate that they do not perform better than these top 2,000 configurations. The best-performing configurations for each instance are provided in Figure 5-6, along with the total travel times and gap associated with the PBIL solutions.

[FIGURE 5 HERE]

[FIGURE 6 HERE]

Most of the best-performing configurations prohibit left turns at the same intersections; intersections with left-turn restrictions applied at that location in at least seven out of nine simulation instances are denoted in Figure 5-6. With only one exception (simulation instance nine), left-turn restrictions are always implemented at the intersections in the central portion of the network. For the lone exception, left turns are restricted at all intersections in the next “ring” of intersections in the central portion of the network. Furthermore, for this exception, the next-best performing configuration that includes left-turn restrictions in the center of the network only has a 0.9% difference in total travel time values. Also, left-turn restrictions are generally more common in the central intersections than those on the periphery. Note, however, that there are some minor differences in these configurations, mostly due to the differences in the realized demands within each simulation instance. For example, left turns are restricted at all central 4×4 intersections in the second simulation instance. However, none of the other simulation instances restrict left turns at all central 4×4 intersections.

For each simulation instance, the PBIL solution also appears to match the best-performing solution obtained from a partial brute-force enumeration quite well. In most cases, only marginal differences exist across the enumeration and PBIL approaches. In simulation instance six, the PBIL-obtained configuration was equal to the best-

performing configuration found using brute-force enumeration. The average difference in total travel time values between PBIL and enumeration solutions is just about 1.9%, which suggests a very good performance of the PBIL algorithm and validates its use for this type of problem.

3.4. *Performance across multiple random seeds*

We now examine the robustness of each configuration across all the simulation instances. This helps to identify a configuration that is robust to minor differences in travel patterns across several days with the same average behaviour. A robust configuration is important to ensure that undesirable outcomes (e.g., high travel times) are not incurred during some days due to minor changes in demand patterns).

Figure 7 shows the total travel time obtained for each simulation instance for the following cases:

- Left-turn restrictions applied at all intersections
- Left-turn restrictions not applied at any intersections
- The configuration obtained using brute-force enumeration for that simulation instance
- The configuration obtained using brute-force enumeration for simulation instance one
- The configuration obtained using PBIL for that simulation instance

The figure reveals that all-or-nothing strategies (left-turn restrictions applied everywhere or nowhere) generally do not perform well compared to the optimized strategies. In general, having no left-turn restrictions increases travel time by about 8% over the best configurations, while restricting left turns at all intersections increases travel time by about 16%. Thus, while previous studies have shown that restricting left turns provides significant benefit under very high demands (Gayah and Daganzo 2012; DePrator, Hitchcock, and Gayah 2017), partial left-turn restrictions within a network can provide a significant benefit under the modest demand scenarios, such as the one used in this paper.

[FIGURE 7 HERE]

Furthermore, as shown by the red-line in Figure 7, the best-performing configuration for the first simulation instance does not perform as well across the other simulation instances. This is because some features of the optimal configuration designed for a specific instance (i.e., demand pattern) might not accommodate other demand patterns very well. Lastly, a comparison of the yellow and blue lines confirm that the PBIL-obtained solution performs well compared to the configuration obtained using brute-force enumeration. In fact, the PBIL obtains the best-performing solution for simulation instance six (though it must be noted that this is a matter of chance).

In light of this, both the brute-force enumeration and PBIL algorithm were used to determine the configuration that performs best under the entire set of simulation instances. In this process, each configuration was tested using all nine simulation random seeds and was scored using the average total travel time observed across all nine instances. The best-performing configuration using the brute-force enumeration and the PBIL algorithm are provided in Figure 8. The performance gap between the two configurations is 1.4%. As expected, the best-performing configurations consist of left-turn restrictions at intersections in the central portion of the network and accommodate left

turns at intersections on the periphery. Across all the simulation instances, the cases in which left turns are accommodated and restricted everywhere have a performance gap of 6.2% and 13.1%, respectively. This also confirms that an all-or-nothing solution does not provide the best network performance across even when evaluated across a set of typical days.

[FIGURE 8 HERE]

4. Tests on imperfect grid networks

The results in the previous section considered the optimal left-turn restriction configuration for a perfect grid network. In this section, the proposed method is applied to an imperfect grid network which might better represent a real-world street network. The network used in this section is created by randomly removing ten links (each representing half of a block) from the perfect grid network while keeping the connectivity between all OD pairs. The network parameters (e.g. link capacity, total demand, jam density, free-flow speed, etc.) are not changed. For the optimization method, the PBIL algorithm is used since it can identify best-performing configurations that are close to (if not equal to) the best solution found in the enumeration runs. Since the new network is not perfectly symmetric, the rotational symmetry constraint for left-turn restriction configurations is also relaxed.

4.1. *Performance of an individual random seed*

The results in this section correspond to a single random seed in the traffic simulation, representing a specific trip generation sequence and OD pattern. Like the analysis of the perfect grid, the PBIL algorithm was run three times to account the inherent randomness of the algorithm. Figure 9 shows the imperfect grid network, left-turn restriction configuration for each optimization run, and their respective total travel time values.

[FIGURE 9 HERE]

The total travel time values of PLT and RLT cases for this network are 4,876,452 and 7,981,897 seconds, respectively. The total travel time difference between PLT and RLT cases for this network is much larger than the perfect grid network. One reason for this is that more turning (both left and right turns) is generally required due to the imperfect nature of the network. As shown in previous sections, the impact or benefit of left turn restriction depends on the left turn volume at the intersections. Since this network has more left turning movements at the intersections, the impact of restricting left turn movement at every intersection is larger for this network. The other reason of greater impact of left turn restrictions for this network is the increased number of detours. Due to the removed links, this network has fewer alternative shortest routes between OD pairs. Thus, restricting left turning movements at every intersection creates more detours resulting in larger total travel time increase. This effect can be seen from the total distance travelled values of PLT and RLT cases for both networks. For this network, RLT configuration increases total distance travelled by 40%. However, for the perfect grid network, the total travel distance increase is around 20%. A similar result can also be observed from the number of left turn restrictions in the configurations obtained by PBIL optimization. The number of restrictions in the PBIL solutions

for this network is smaller than the PBIL solutions for the perfect grid network. The changes in the network also affected the resulting spatial configuration of left-turn restrictions. As seen from Figure 9, there are five common left turn restriction locations across three PBIL runs. Like the results of perfect grid network, these locations are generally located in the central part of the network. However, unlike the previous results, left turn restrictions are also enacted on the periphery of the network. These intersections and the intersections that are not left turn restricted in the central part of the network are the result of the different routing behaviours of the imperfect grid network, which can be seen in Figure 10. Compared to the perfect grid network, some links on the periphery of the imperfect grid network have a significantly larger total volume, and some intersections in the central area have a larger ratio of left turning vehicles. Additionally, left-turn restrictions are not enacted at all central intersections since doing so might cause one or more OD pairs not to have a feasible route between them.

[FIGURE 10 HERE]

Nevertheless, the network configuration identified by the PBIL algorithm performs better than either of the all-or-nothing approaches. Examination of Figure 10 confirms that these restrictions tend to occur at intersections that carry higher total flows or serve fewer left-turning vehicles (relative to through vehicles).

4.2. *Performance of multiple random seeds*

We now examine the robustness of obtained solutions across multiple simulation instances. The PBIL algorithm was run using six different random seeds (i.e., six different instances of OD patterns and trip generation sequences). Figure 11 shows the total travel time values for the left turn restriction configurations of PLT, RLT, and PBIL solution for each random seed. Like the results of the perfect grid network, the results shown in Figure 11 suggest that partial left turn restrictions can provide significant benefits under modest demands. As seen from Figure 11, the PBIL-obtained configurations perform better than PLT and RLT networks in all cases. On average, best-performing PBIL configurations decrease total travel time by 12% and 46% over PLT and RLT networks, respectively.

[FIGURE 11 HERE]

The common left turn restriction locations of three PBIL runs with single random seed (Figure 9) can also be observed in the results of PBIL runs with different random seeds. Figure 12 shows the best-performing configurations found from PBIL algorithm for each random seed.

[FIGURE 12 HERE]

All six of the best-performing configurations share a similar pattern of left-turn restriction locations at the center of the network. For all simulation instances, left-turning movement in the central 2×2 section of the network is not restricted, and the left-turn restricted intersections in the central 4×4 part of the network are reasonably similar. However, there is no emerging pattern for the periphery of the network, mostly due to the inherent randomness of microsimulation and PBIL algorithm.

5. DISCUSSION AND CONCLUDING REMARKS

This study examined the effectiveness of a population-based incremental algorithm to identify the optimal spatial configuration of left-turn restrictions within both perfect and imperfect square grid networks. Network performance under different configurations was tested using the Aimsun micro-simulation platform to accurately model traffic dynamics such as queue spillbacks and gap acceptance behaviour. Each intersection was provided with a choice of accommodating left turns through permitted phasing or restricting left turns altogether. Although this is a binary decision at each individual intersection, determining the optimal configuration is a complex combinatorial optimization problem due to the large number of intersections for which this decision must be made and the interdependence in operation of nearby intersections. Comparison with a brute-force enumeration of a subset of potential feasible options reveals that the PBIL algorithm is able to successfully identify configurations that perform close to the optimal configuration. The PBIL algorithm also significantly reduces the computational time. The computational time needed for evaluation of a single LT restriction configuration is approximately 8 seconds on a computer with 4-core 5th generation Intel i7 CPU. Thus, a brute force enumeration of all possible LT-restriction configurations for an 8x8 network can take about 10^{12} years (2^{64} configurations \times 8 seconds). The proposed algorithm finds a reasonably good solution by evaluating 1600 LT restriction configurations in less than four hours.

The best-performing configurations obtained from analysis of square grid networks can reveal generalizable insights on how left-turn restrictions should be spatially implemented on more realistic urban traffic networks. For example, the results on the perfect grid case (assuming configurations should be rotationally symmetric to match the symmetric network structure and demand pattern) suggest that left-turn restrictions should generally be enacted at central intersections where flows are highest, in order to take advantage of the increased intersection capacity that these restrictions provide. Vehicles passing through these central intersections generally have alternative routes available to them, which limits the increased travel distance incurred by implementing the left-turn restrictions. By contrast, left-turn restrictions should not be enacted at intersections on the periphery of the network: doing so would impact more vehicles, since a higher fraction of vehicles turn left at intersections on the periphery than at intersections in the center, and the additional capacity brought by left-turn restrictions generally goes unused since these intersections carry lower flows. These results are consistent over individual simulation instances, even though there are minor differences due to the realized demands in each instance. Additional simulation tests also show that these trends continue to hold even when the rotational symmetry assumption is relaxed. In imperfect grids (where the no symmetry assumptions are made), the general trends still hold that left-turn restrictions should be enacted at locations with high flows and low ratio of left-turning vehicles; however, there are obvious cases where a high flow of vehicles would need to make a left turn to access a specific destination.

The results suggest that restricting left turns selectively at a subset of locations can provide a significant travel time savings with modest negative outcomes (e.g., increases in travel distances). For example, restricting left turns at all intersections increases travel distance by approximately 32.2%. By contrast, the optimal configuration that minimizes travel times increases travel distance by just 9.1% but offers a travel time savings of 8.7%. To put this in perspective, a recent study (Boyles, Rambha, and Xie 2015) compared the use of a low-conflict vortex design (Eichler, Bar-Gera, and

Blachman 2013) with one-way and two-way grids. The results suggested that the vortex configuration would reduce travel time compared with the two-way grid (with left turns) by 53.5% but require an increase in total travel distance of by 25.4%. The use of one-way grids, by contrast, could reduce travel times by 15.4% but would increase travel distances by 5.6%. However, these latter statistics were obtained using a static network assignment algorithm that does not consider the impact of queue spillovers and more realistic traffic dynamics, and thus they might not be directly comparable to the values obtained in this work. Nevertheless, the results of this work suggest that operational improvements in terms of travel time can be obtained in grid networks with less radical strategies than moving to one-way grids or vortex intersections by simply banning left turns selectively in a network.

Of course, the optimal spatial configuration of left-turn restrictions would be subject to site-specific features, such as network structure and demand patterns. Before implementation, potential configurations should be thoroughly tested to ensure that it would improve operational performance. However, the general trends of this work are likely to hold such that the best-performing configuration identified here provides a good starting point that could be modified due to these site-specific features. Specifically, left-turn restrictions should be specifically considered at locations that currently carry the largest flows and with the smallest left-turning ratios so that the additional capacity can be leveraged without causing many vehicles to detour and travel additional distance. And, the PBIL algorithm can be readily implemented to the structure of more realistic network structures using the methods proposed here. The future work will consider incorporating local search methods and possible site-specific constraints (e.g. symmetry constraint) to improve the optimization process. Further work should also consider how these central left-turn restrictions might influence overall network resilience to disruptions that might occur along links, such as traffic crashes or bottlenecks caused by freight vehicles. The proposed PBIL method can also be applied to identify optimal location of other traffic control strategies, such as transit signal priority, bus lanes or other features.

Disclosure statement

The authors of this manuscript certify that they have no affiliations with or involvement in any organization or entity with any financial interest, or non-financial interest in the subject matter or materials discussed in this manuscript.

Acknowledgments

This research was supported by NSF Grant CMMI-1749200

Notes on contributors

Vikash V. Gayah received the B.S. and M.S. degrees in civil and environmental engineering from University of Central Florida, Orlando, FL, USA, and the Ph.D. degree in civil and environmental engineering from University of California, Berkeley, CA, USA. He currently serves as an Associate Professor with the Department of Civil and Environmental Engineering, The Pennsylvania State University (Penn State), University

Park, PA, USA. His research interests include macroscopic modeling of urban transportation systems, traffic operations and control, public transportation, and traffic safety.

Murat Bayrak received a M.S. degree in 2016 in civil engineering from the Bogazici University, Istanbul, Turkey, and the Ph.D. degree in civil and environmental engineering from the Pennsylvania State University, University Park, PA, USA. He is currently a postdoctoral researcher with the Department of Built Environment, Aalto University, Finland. His research interests include transit priority applications, public transportation planning, and traffic operations and control.

Zhengyao Yu received the M.S. and Ph.D. degrees in civil engineering from the Pennsylvania State University, University Park, PA, USA. He is currently a data scientist at Verizon Wireless. His research interests include urban transportation network modeling and advanced traffic control systems.

References

Baluja, Shumeet. 1994. *Population-based incremental learning. a method for integrating genetic search based function optimization and competitive learning*. Report. Carnegie-Mellon Univ Pittsburgh Pa Dept Of Computer Science.

Berkowitz, Carl, Clifford Bragdon, and Francisco Mier. 1996. "Continuous flow intersection: A public private partnership." In *IEEE Vehicle Navigation and Information Systems Conference*, Orlando, USA, October 14-18, 277–287.

Boyles, S. D., T. Rambha, and C. Xie. 2015. "Equilibrium analysis of low-conflict network designs." *Transportation Research Record* (2467): 129–139.

Chowdhury, M., N. Derov, P. L. Tan, and A. Sadek. 2005. "Prohibiting left-turn movements at mid-block unsignalized driveways: Simulation analysis." *Journal of Transportation Engineering* 131 (4): 279–285.

Chowdhury, Md Shoaib. 2011. "An Evaluation of New Jersey Jug-Handle Intersection (NJJ) With and Without Pre-Signals." In *Transportation and Development Institute Congress 2011: Integrated Transportation and Development for a Better Tomorrow*, Chicago, USA, March 13-16, 1245–1254.

Cottrell, Benjamin H. 1985. *Guidelines for Protected Permissive Left Turn Signal Phasing*. Virginia Highway and Transportation Research Council.

Daganzo, C. F. 2007. "Urban gridlock: Macroscopic modeling and mitigation approaches." *Transportation Research Part B-Methodological* 41 (1): 49–62.

Daganzo, C. F., V. V. Gayah, and E. J. Gonzales. 2011. "Macroscopic relations of urban traffic variables: Bifurcations, multivaluedness and instability." *Transportation Research Part B-Methodological* 45 (1): 278–288.

DePrator, A. J., O. Hitchcock, and V. V. Gayah. 2017. "Improving Urban Street Network Efficiency by Prohibiting Conflicting Left Turns at Signalized Intersections." *Transportation Research Record* (2622): 58–69.

Eichler, D., H. Bar-Gera, and M. Blachman. 2013. "Vortex-based zero-conflict design of urban road networks." *Networks and Spatial Economics* 13 (3): 229–254.

Fambro, Daniel B, Carroll J Messer, and Donald A Andersen. 1977. "Estimation of unprotected left-turn capacity at signalized intersections." *Transportation research record* 644: 113–119.

Gayah, V. V., and C. F. Daganzo. 2011. "Clockwise hysteresis loops in the Macroscopic Fundamental Diagram: An effect of network instability." *Transportation Research Part B-Methodological* 45 (4): 643–655.

Gayah, V. V., and C. F. Daganzo. 2012. "Analytical Capacity Comparison of One-Way and Two-Way Signalized Street Networks." *Transportation Research Record* (2301): 76–85.

Gayah, V. V., X. Y. Gao, and A. S. Nagle. 2014. "On the impacts of locally adaptive signal con-

trol on urban network stability and the Macroscopic Fundamental Diagram.” *Transportation Research Part B-Methodological* 70: 255–268.

Girault, J. T., V. V. Gayah, S. I. Guler, and M. Menendez. 2016. “An Exploratory Analysis of Signal Coordination Impacts on the Macroscopic Fundamental Diagram.” *Transportation Research Record* 2560: 36–46.

Haddad, Jack, and Nikolas Geroliminis. 2013. “Effect of left turns for arterials with queue spillbacks.” In *92nd Annual Meeting of the Transportation Research Board*, Washington, D.C., January 13-17.

Hajbabaie, Ali, Juan C Medina, and Rahim F Benekohal. 2010. “Effects of ITS-based left turn policies on network performance.” In *13th International IEEE Conference on Intelligent Transportation Systems*, Funchal, Portugal, September 19-22, 80–84.

Hughes, Warren, Ram Jagannathan, Dibu Sengupta, and Joe Hummer. 2010. *Alternative intersections/interchanges: informational report (AIIR)*. Report. United States. Federal Highway Administration.

Hummer, Joseph E. 1998. “Unconventional left-turn alternatives for urban and suburban arterials—part two.” *ITE journal* 68 (11): 101–106.

Knoop, V. L., S. P. Hoogendoorn, and J. W. C. Van Lint. 2012. “Routing Strategies Based on Macroscopic Fundamental Diagram.” *Transportation Research Record* (2315): 1–10.

Liu, Y., and Z. K. Luo. 2012. “A bi-level model for planning signalized and uninterrupted flow intersections in an evacuation network.” *Computer-Aided Civil and Infrastructure Engineering* 27 (10): 731–747.

Long, J. C., W. Y. Szeto, and H. J. Huang. 2014. “A bi-objective turning restriction design problem in urban road networks.” *European Journal of Operational Research* 237 (2): 426–439.

Mazloumian, A., N. Geroliminis, and D. Helbing. 2010. “The spatial variability of vehicle densities as determinant of urban network capacity.” *Philosophical Transactions of the Royal Society a-Mathematical Physical and Engineering Sciences* 368 (1928): 4627–4647.

Messer, Carroll J, and Daniel B Fambro. 1977. “Effects of signal phasing and length of left-turn bay on capacity.” *Transportation Research Record* (2315): 95–101.

Newell, Gordon F. 1959. “The effect of left turns on the capacity of a traffic intersection.” *Quarterly of Applied Mathematics* 17 (1): 67–76.

Ortigosa, J., V. V. Gayah, and M. Menendez. 2019. “Analysis of one-way and two-way street configurations on urban grid networks.” *Transportmetrica B-Transport Dynamics* 7 (1): 61–81.

Ortigosa, J., and M. Menendez. 2014. “Traffic performance on quasi-grid urban structures.” *Cities* 36: 18–27.

Ortigosa, J., M. Menendez, and V. V. Gayah. 2015. “Analysis of Network Exit Functions for Various Urban Grid Network Configurations.” *Transportation Research Record* (2491): 12–21.

Reeves, Colin R, and Christine C Wright. 1995. “Epistasis in Genetic Algorithms: An Experimental Design Perspective.” In *6th International Conference on Genetic Algorithms*, Pittsburgh, USA, July 15-19, 217–224.

Reid, Jonathan D, and Joseph E Hummer. 2001. “Travel time comparisons between seven unconventional arterial intersection designs.” *Transportation Research Record* 1751 (1): 56–66.

Roess, Roger P, Elena S Prassas, and William R McShane. 2010. *Traffic engineering*. 4th ed. Pearson/Prentice Hall.

Saberi, Meead, Hani S Mahmassani, and Ali Zockaie. 2014. “Network capacity, traffic instability, and adaptive driving: findings from simulated urban network experiments.” *EURO Journal on Transportation and Logistics* 3 (3-4): 289–308.

Tang, Q. 2019. “Minimization of road network travel time by prohibiting left turns at signalized intersections.” PhD diss., Technische Universität Braunschweig.

Tang, Q., and B. Friedrich. 2016. “Minimization of travel time in signalized networks by prohibiting left turns.” *Transportation Research Procedia* 14: 3446–3455.

Tang, Q., and B. Friedrich. 2018. "Design of signal timing plan for urban signalized networks including left turn prohibition." *Journal of Advanced Transportation* 2018.

Tang, Q., H. Liu, and B. Friedrich. 2019. "Lane-based signal optimization with left turn prohibition in urban road networks." *Canadian Journal of Civil Engineering* 46 (2): 73–80.

Xuan, Y. G., C. F. Daganzo, and M. J. Cassidy. 2011. "Increasing the capacity of signalized intersections with separate left turn phases." *Transportation Research Part B-Methodological* 45 (5): 769–781.

Xuan, Yiguang, Vikash V Gayah, Michael J Cassidy, and Carlos F Daganzo. 2012. "Presignal Used to Increase Bus-and Car-Carrying Capacity at Intersections: Theory and Experiment." *Transportation research record* 2315 (1): 191–196.

Yu, Z., and V. V. Gayah. 2018. "Comparison of Urban Street Network Resilience for Grid Networks with and Without Left-Turning Maneuvers Under Light Traffic Situations." In *97th Annual Meeting of the Transportation Research Board*, Washington, D.C., January 7-11.

Yu, Z., and V. V. Gayah. 2019. "Network Performance under Link Disruptions: A Comparison of Two-Way and One-Way Network Configurations." In *98th Annual Meeting of the Transportation Research Board*, Washington, D.C., January 13-17.

Zhao, J., Y. Liu, and T. Wang. 2016. "Increasing signalized intersection capacity with unconventional use of special width approach lanes." *Computer-Aided Civil and Infrastructure Engineering* 31 (10): 794–810.

Zhao, J., W Ma, H. M. Zhang, and X. Yang. 2013. "Increasing the capacity of signalized intersections with dynamic use of exit lanes for left-turn traffic." *Transportation Research Record* (2355): 49–59.

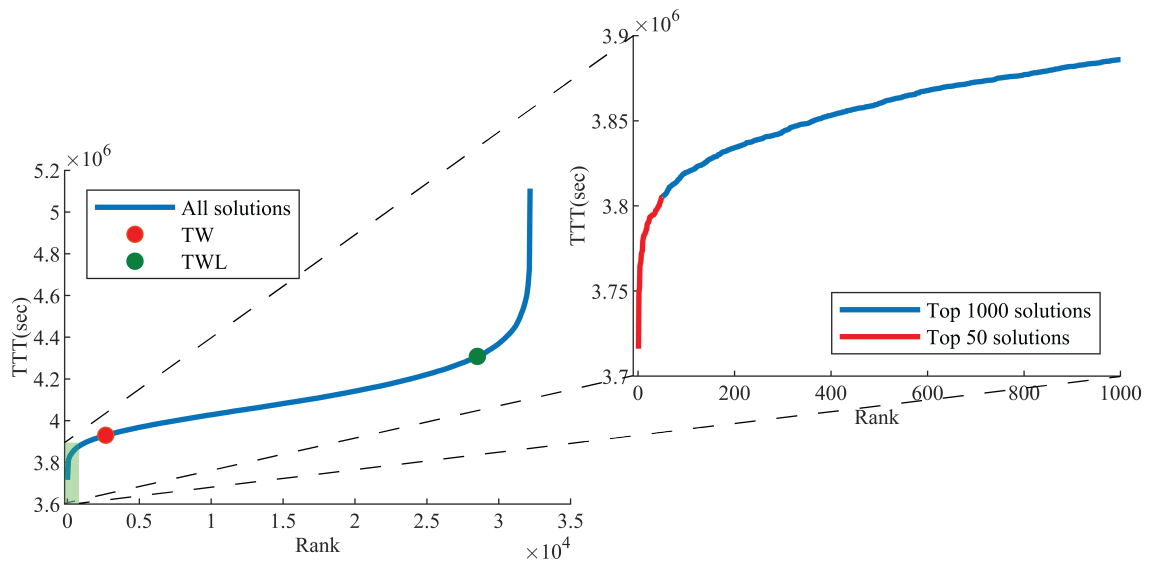


Figure 1. Ranking of all left-turn restriction configurations based on total travel time

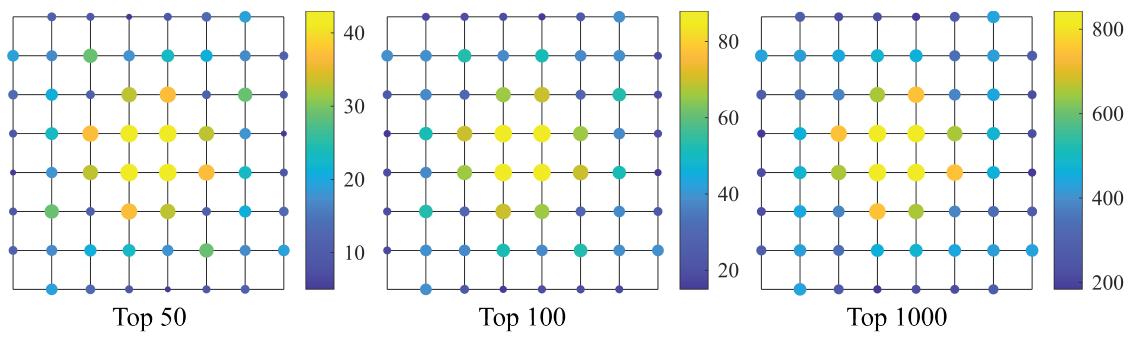


Figure 2. Heat map showing common features of top-performing 50, 100 and 1000 left-turn restriction configurations

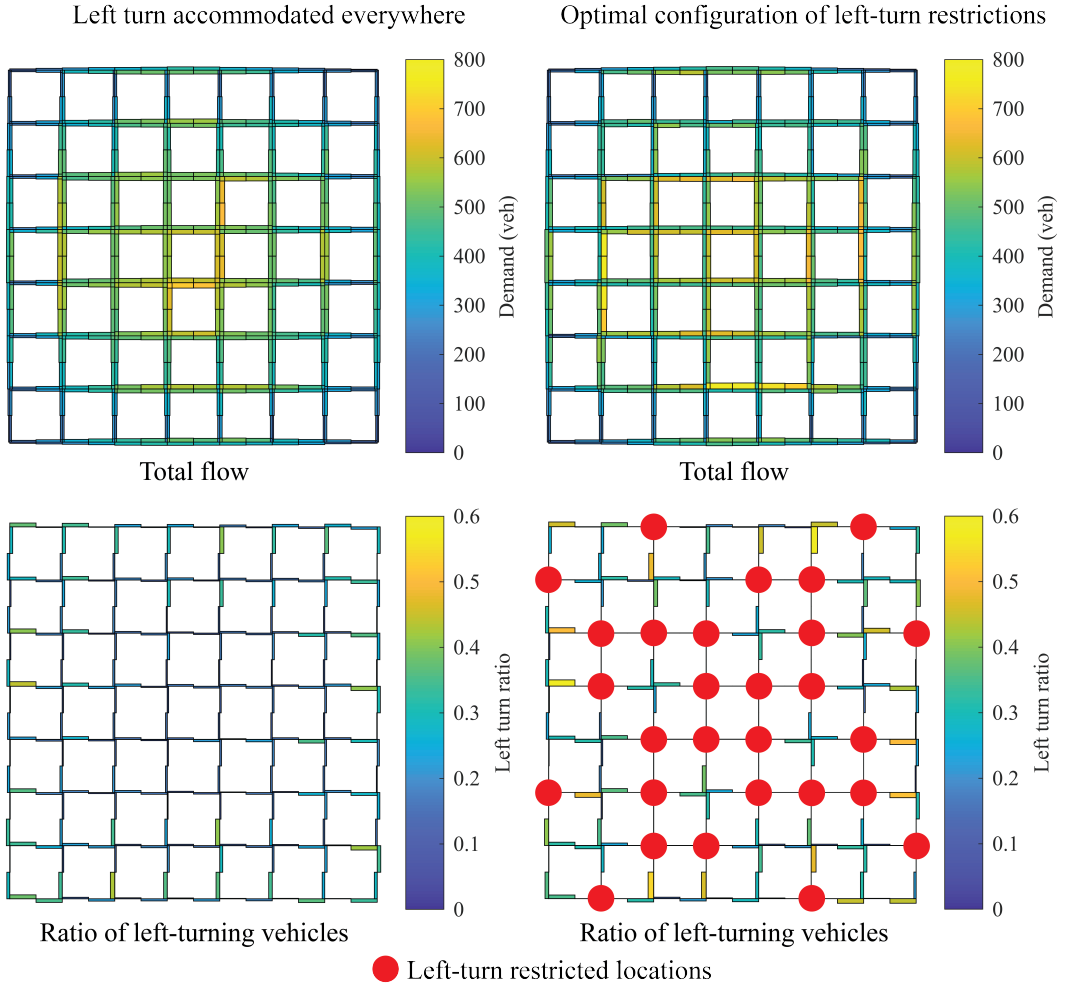


Figure 3. Heat map showing total vehicle flow and left-turning ratio along all links in the network for PLT and optimum configurations.

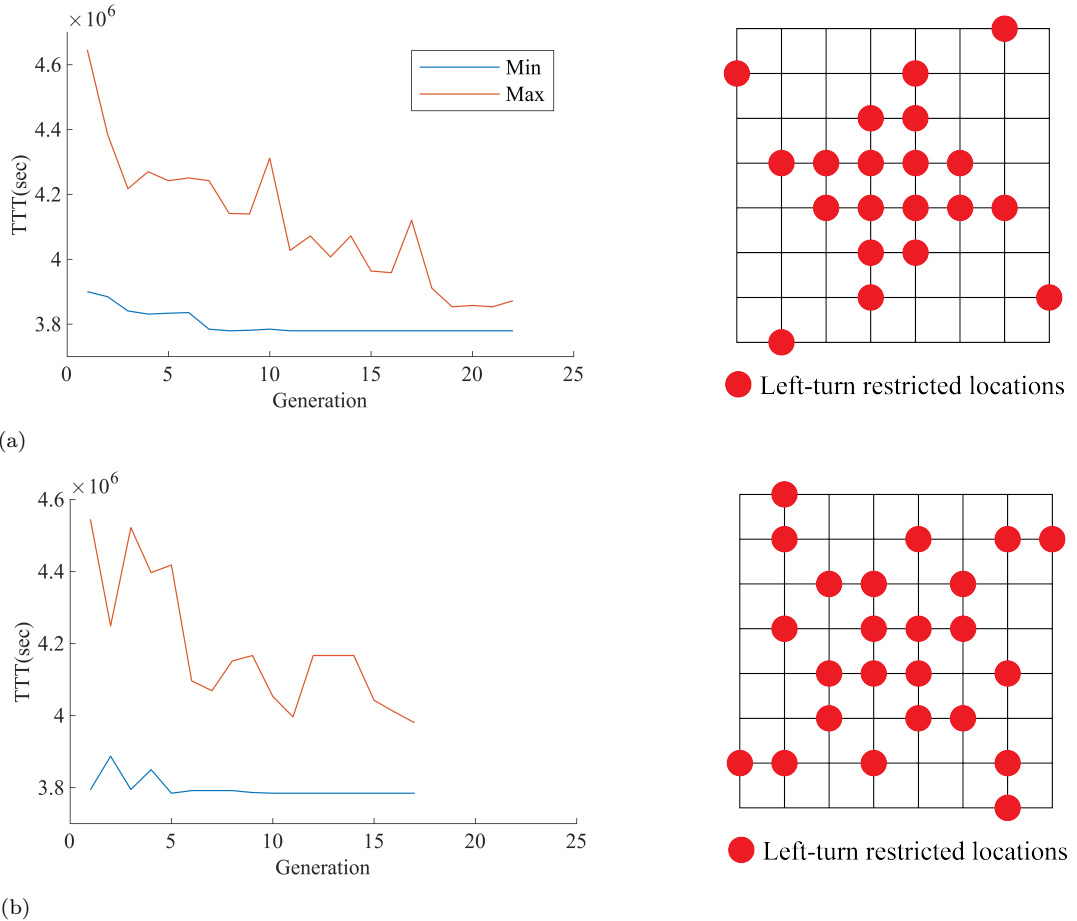


Figure 4. Illustration of solution convergence (left) and left-turn restriction configuration (right) for (a) first PBIL instance and (b) second PBIL instance.

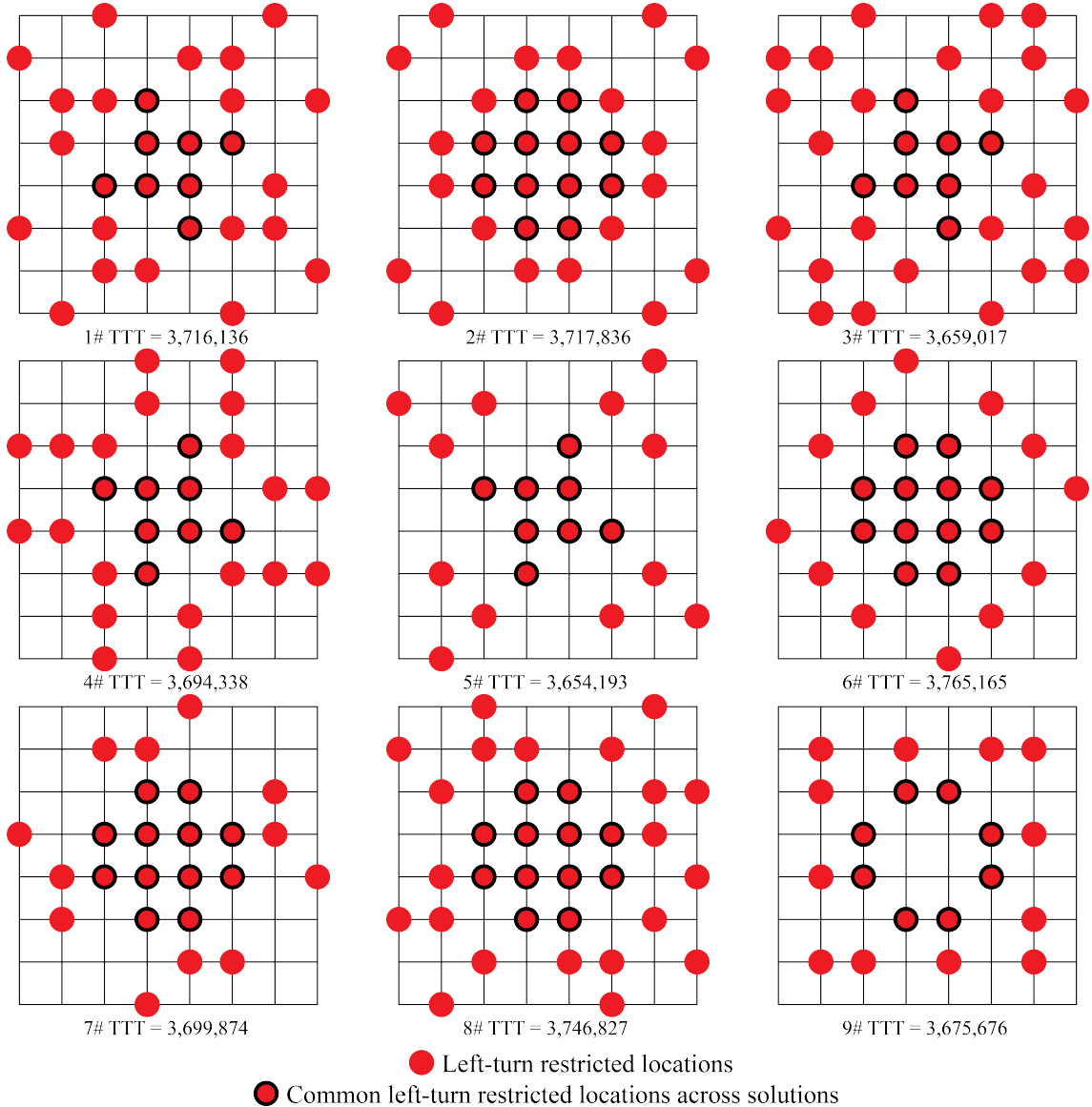


Figure 5. Best-performing configurations for the set of nine simulation instances obtained from enumeration of top-performing solutions

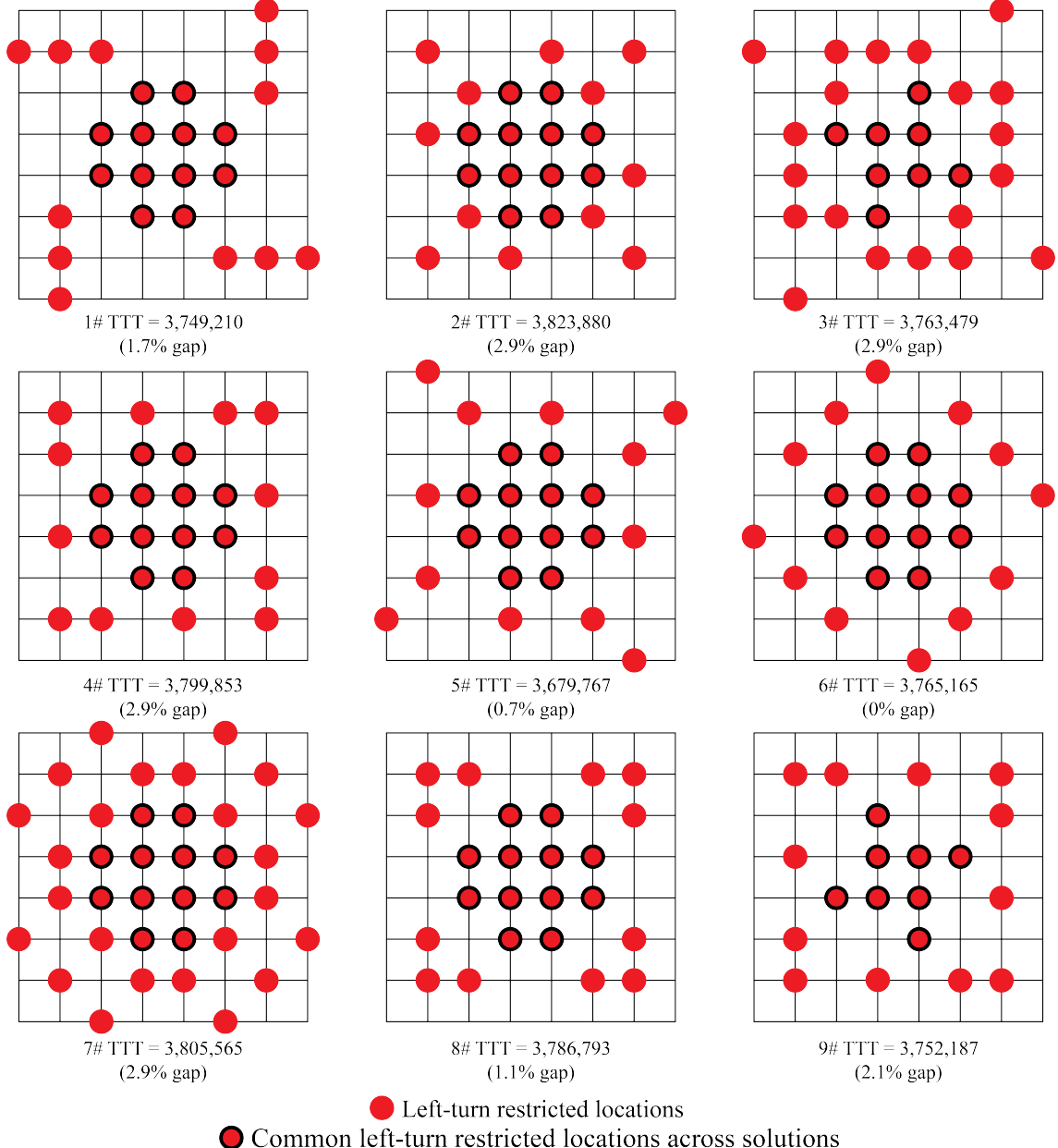


Figure 6. Best-performing configurations for the set of nine simulation instances obtained from PBIL algorithm.

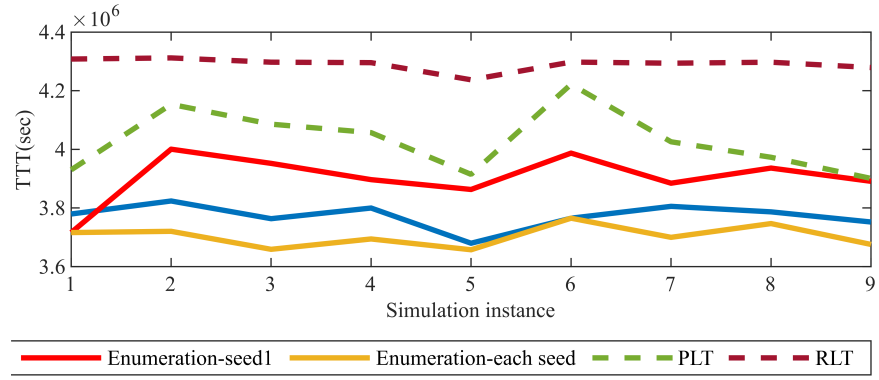


Figure 7. Total travel time obtained for various simulations instances and left-turn restriction configurations.

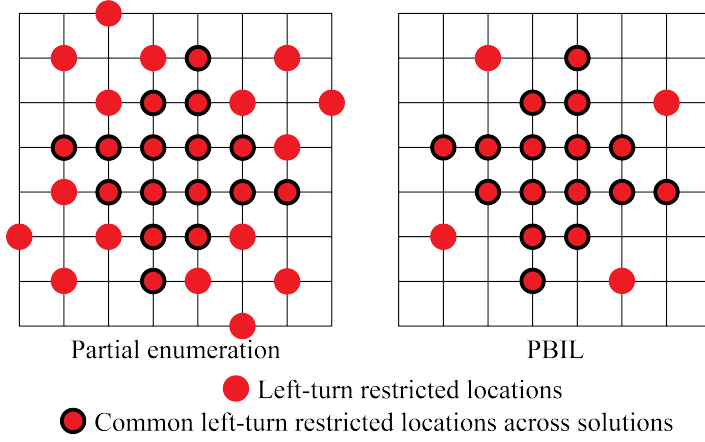


Figure 8. Best-performing left-turn restriction configuration across all nine simulation instances obtained (a) using partial enumeration of solutions and (b) using the PBIL algorithm.

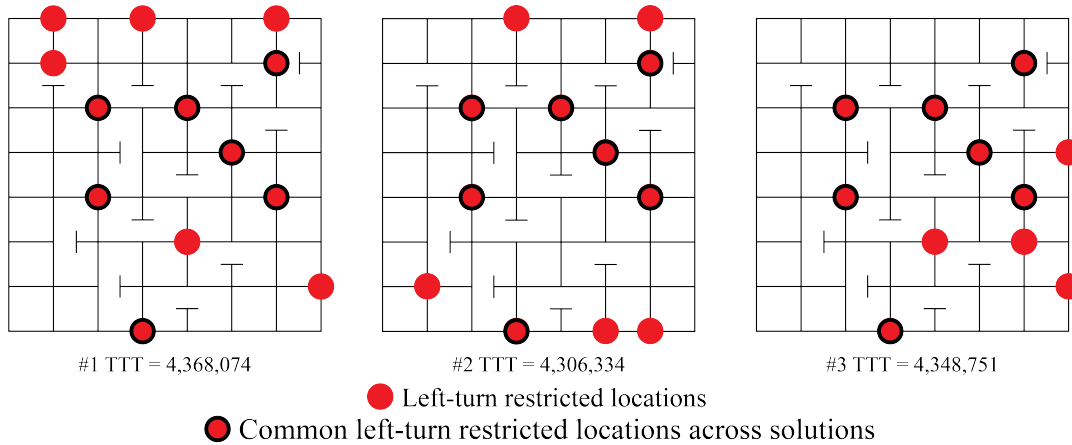


Figure 9. Left-turn restriction configurations and total travel time values for three simulation instances obtained from PBIL algorithm.

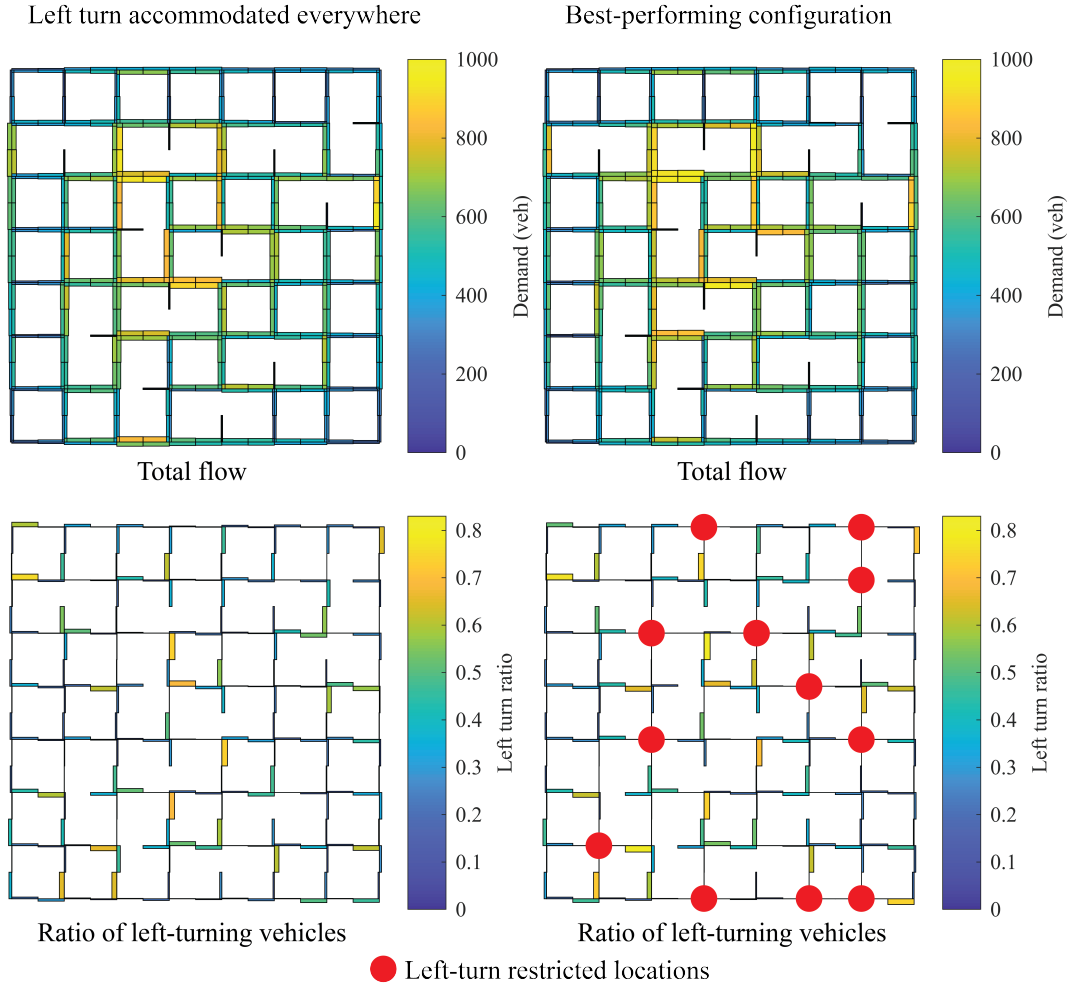


Figure 10. Heat map showing total vehicle flow and left-turning ratio along all links in the network for PLT and optimum configurations.

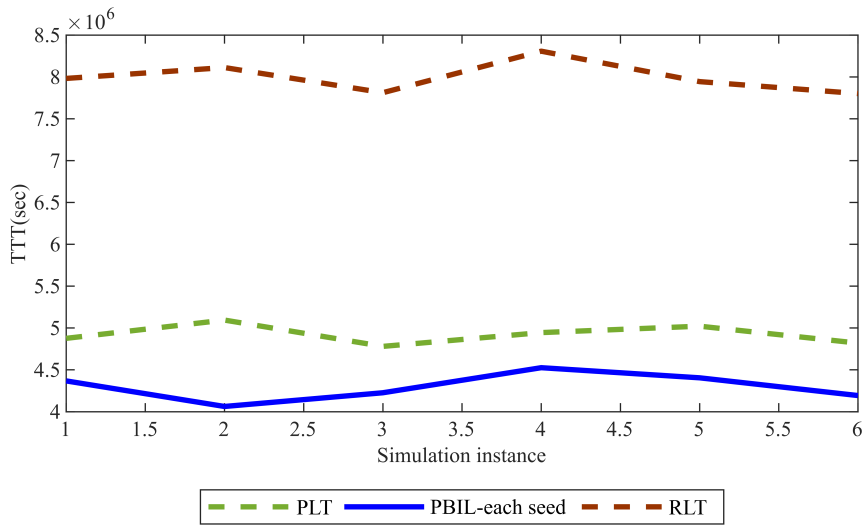


Figure 11. Total travel time obtained for various simulations instances and left-turn restriction configurations.

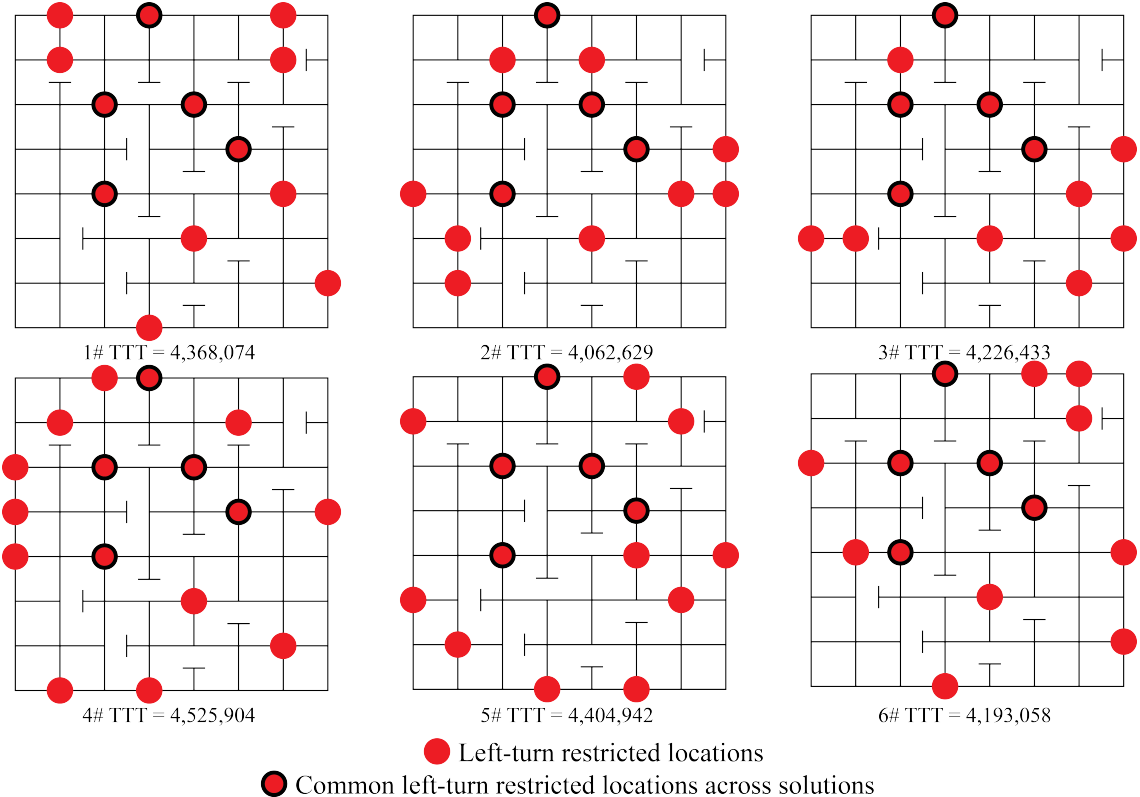


Figure 12. Best-performing configurations for the set of six simulation instances obtained from PBIL algorithm.